Application Note

High Definiton Kelvin Force Microscopy
BIMODAL HD-KFM

INTRODUCTION

Since the invention of the Atomic Force Microscope in 1986, many different measurement modes have been proposed to characterize other interaction forces or surface properties in addition to the topography.

An example of this could be: magnetic field (MFM), electric field (EFM), nanoscale dissipation processes (Force Modulation, phase imaging, Force spectroscopy), thermal conductivity (Scanning Thermal–AFM), electrical conductivity (Conductive-AFM), resistance (ResiScope),surface potential (KFM), piezo response (PFM), Young's modulus (Force spectroscopy),…

Additionally, it can be used in ambient conditions, liquid environment, ultra-high vacuum, temperature gradients or low temperature.

One of the most interesting applications of AFM is nano-electric characterization, this is the capability tomeasure electric properties with nanometre lateral resolution. This is of great interest for the development of so called nano-materials. The emergence of 2-D materials like graphene, molybdenum disulphide or black phosphorous has created an interest in characterizing and understanding the electrical properties of flakes with one or multiple layers.

In the field of solar cells and piezoelectric materials, there is also a growing interest in perovskite type materials as they show promising percentages of light efficiency conversion.

There are also other fields of materials science or biology, where nano-electrical properties are of high interest.

One of the most popular electrical modes of AFM is the Kelvin Force Mode (KFM) or Kelvin Probe Atomic Force Microscopy (KP-AFM), in fact the same technique can be found in literature with slightly different names or acronyms. This technique allows measurement of the surface potential between the tip of the AFM and the surface which can be related to material properties like the work function or the bandgap.

Although Kelvin Probe is a technique known since 1898, it was a few years after the invention of AFM that a conductive probe was first combined with AFM to provide nanometric resolution.

More interestingly, since the apparition of KFM, two different approaches have been used to implement it.

One is based on what is typically referred to as the double-pass technique (or lift-mode technique) and the other is usually referred to as the single-pass KFM technique. It is important then to describe the background theory of KFM in order to distinguish between these two approaches.

It is also important to describe a further advancement of single-pass KFM: Bimodal HD-KFM. This technique has been developed by Concept Scientific Instruments exclusively for the Nano-Observer AFM.

BACKGROUND THEORY OF KELVIN PROBE FORCE MICROSCOPY

The KFM technique combines oscillating mode AFM and the Kelvin probe technique. In this mode, both a DC bias (V_{DC}) and an oscillating bias (V_{AC}) are applied between tip and sample. The interaction force in this operation mode can be mathematically described by considering the tip-sample as a capacitor:

$$F_{electric} = -\frac{1}{2}\frac{\partial C}{\partial z}V^2 = -\frac{1}{2}\frac{\partial C}{\partial z}[V_{DC} - V_{POTENTIAL} + V_{AC}sin(\omega_{AC}t)]^2 \quad (1)$$

where C is the capacitance, z is the relevant spatial direction and $V_{POTENTIAL}$ is the contact potential difference between tip and sample:

$$V_{POTENTIAL} = \frac{\Delta\varphi}{e} = \frac{\varphi_{tip} - \varphi_{sample}}{e} \quad (2)$$

Where Ø is the work function and e is the electron charge.

By using a tip with a known work function (typically tips coated with Pt) the work function of the sample can be measured.

By developing the squared terms, the interaction force can be separated into several components

$F_{electric} = F_{DC} + F_{AC} + F_{2AC}$:

$$F_{DC} = -\frac{\partial C}{\partial z}\left[(V_{DC} - V_{POTENTIAL})^2 + \frac{V_{AC}^2}{4}\right] \quad (3)$$

$$F_{AC} = -\frac{\partial C}{\partial z}[(V_{DC} - V_{POTENTIAL})V_{AC}sin(\omega_{AC}t)] \quad (4)$$

$$F_{2AC} = \frac{\partial C}{\partial z}\frac{V_{AC}^2}{4}cos(2\omega_{AC}t) \quad (5)$$

Thus, by applying an electric excitation to the cantilever at a certain frequency V_{AC}, the cantilever will oscillate at that the same frequency with a certain amplitude A_{AC} and at twice the excitation frequency of V_{AC} with an amplitude A_{2AC} due to the F_{AC} and F_{2AC} components described in (4) and (5).

A particular situation is achieved when V_{DC} bias is tuned so it equals $V_{POTENTIAL}$: the F_{AC} component becomes zero and so it does A_{AC} (cantilever does not oscillate at that frequency). By implementing a feedback loop on the A_{AC} amplitude with V_{DC} as the actuation signal, $V_{POTENTIAL}$ over the surface can be mapped by constantly nullifying A_{AC} during the scan.

As mentioned above there are two different ways to implement KFM: KFM double pass and KFM single pass. Additionally, KFM can be implemented with the feedback signal operating on the oscillating amplitude of the cantilever (AM-KFM) or in the oscillating frequency (FM-KFM). In this application note we will focus on the first case.

It is important to notice that in KFM mode, as in EFM or MFM mode, there are two main contributions to the total force acting on the tip:
1) Surface interaction (this is the short-range topography-related interaction force and the long range Van der Waal type forces).
2) Long range electrostatic contribution, arising from the surface potential and the applied bias.
In the KFM mode double-pass implementation, both contributions are decoupled through the lift height separation in the second pass (also known as lift mode technique).
In the KFM mode single-pass implementation, both contributions are decoupled through the use of a multi-frequency approach. This approach requires a simultaneous excitation of the cantilever at two different frequencies. Typically, the topography is tracked by exciting mechanically the cantilever at its first eigenmode resonance frequency and using a feedback operating with the mechanical amplitude.
The second feedback is operated on the amplitude of the electrical oscillation of the cantilever at a different frequency.
One of the clear advantages of the single-pass approach as compared to the double pass implementation is the enhancement of resolution and sensitivity as the tip remains in the non-contact regime, but also much closer to the surface as illustrated in Figure 1.
A direct comparison between both techniques is made on a graphene sample over a SiC substrate. The contact potential image obtained in single-pass setup provides better contrast and lateral resolution of the graphene domains. This is due to the fact that in a single-pass approach, the tip is oscillating closer to the surface (typically 0.1 nm-0.3 nm or touching the surface intermittently) as compared to the double-pass mode or lift mode (typically 10 nm-20 nm).
As the electric field decays with the separation distance, standard double-pass has an intrinsic loss of sensitivity and lateral resolution.

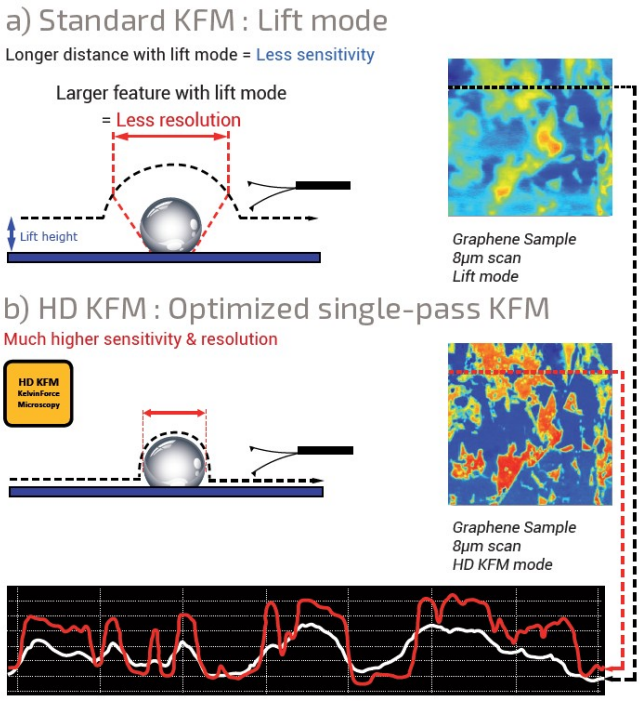

Figure 1: Comparison between standard double-pass and Bi-modal HD-KFM.

KFM MODE IN DOUBLE PASS MODE (LIFT MODE)

KFM can be implemented by means of the Lift Mode technique (or commonly named as "Double pass KFM"). In this technique, the cantilever scans the same line twice by means of the lift mode technique.

The lift mode technique is also implemented in the Nano-Observer AFM to perform electric and magnetic measurements in an ease of use design.
The lift mode technique allows us to easily decouple long range interactions (electric and magnetic typically) from surface interactions by performing two consecutive scans over the same line of the substrate.

Figure 2 shown how KFM is operated with the lift mode technique:

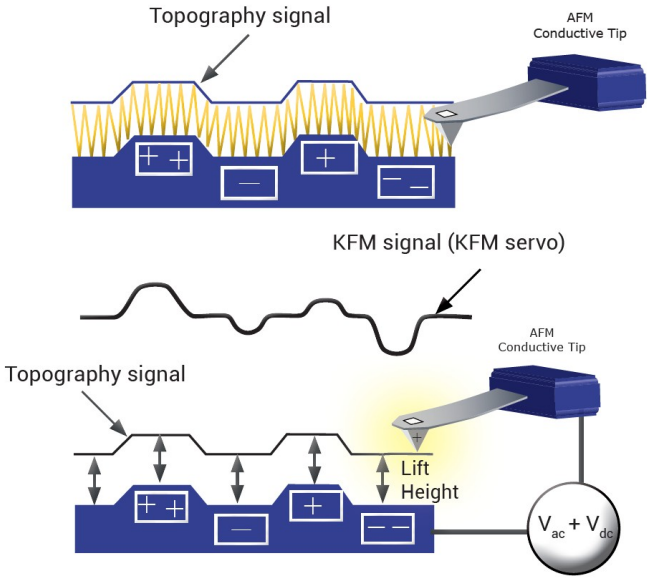

Figure 2: Implementation of KFM with dual-pass/lift-mode technique.

In the first line scan (Fig. 2-top), the cantilever oscillates close to the sample as in standard oscillating mode without bias applied. In these conditions, the tip tracks topography of the surface (black dashed lines modulating the oscillating amplitude)

In the second line scan (Fig. 2-bottom), the cantilever oscillates at a certain separation distance (known as lift height) following the topography measured in the first scan.
By operating in this manner the separation distance is kept constant.
During this second scan, an electric bias VAC is applied between tip and sample. Oscillation amplitude due to this bias is used for the electric feedback to operate. An additional DC bias VDC is applied by the KFM feedback to nullify the electric amplitude oscillation.

Traditionally, double-pass KFM was implemented to work in air conditions in the intermittent contact regime to avoid instabilities from the adhesion to the surface. In that manner, by controlling the lift height, working in a non-contact regime could be accomplished easily.

KFM MODE IN SINGLE-PASS MODE

As mentioned above, a single pass technique requires two independent feedbacks operating at different frequencies of the cantilever. The main goal to implement a single-pass KFM is to properly tune the lock-in and the feedback-loop which require some expertise to properly nullify the electrostatic interaction.

Although traditional approaches in single-pass implementation worked with the electric feedback operating at frequencies much lower than the mechanical frequency (typically < 20 kHz) there have been some recent improvements in the algorithm which enhances the concept of single-pass from standard to «Bimodal HD-KFM», where HD stands for High-Definition due to the improvement in the sensitivity and resolution.

HD-KFM. THE MOST ADVANCED SINGLE-PASS KFM MODE

On the contrary to standard single-pass setups, Bimodal HD-KFM is characterized because the electric feedback is tuned to the second eigenmode frequency of the cantilever.

Fig. 3 shows the concept on which HD-KFM is based: the first flexural eigenmode of the cantilever is excited mechani-cally and the second flexural mode is excited electrically. In the past decade, multi-frequency approach has become one of the front-end topics amongst the AFM community as it has shown many potential applications.

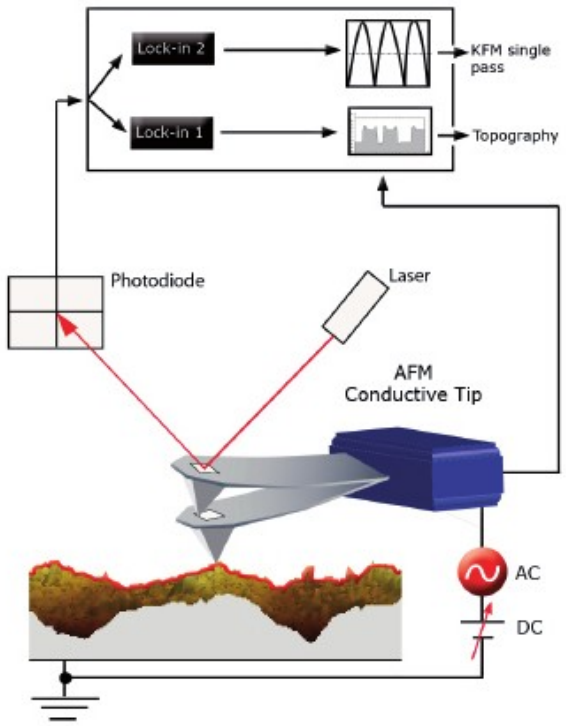

Figure 3: schematics of Bimodal HD-KFM setup

The advantages of tuning the V_{AC} bias used for the electric feedback to the second eigenmode of the cantilever is that the signal is amplified by the Q factor of the second eigen-mode. This effect provides the possibility to use smaller V_{AC} values to obtain an oscillation amplitude with an acceptable signal to noise ratio as compared to other implementations not-based on the second eigenmodeamplification. Additionally, stiffer effective spring constant of the second eigenmode provides more stability of the oscillation during the scanning of the surface.

In Fig. 4, it is shown an schematics of the HD-KFM setup implementation with the electric diagram of HD-KFM where the first flexural mode is excited mechanically and the second flexural mode is excited electrically.

The topographic feedback operates on the mechanical amplitude (lock-in 1) and the electrical feedback operates on the electric amplitude (lock-in 2).

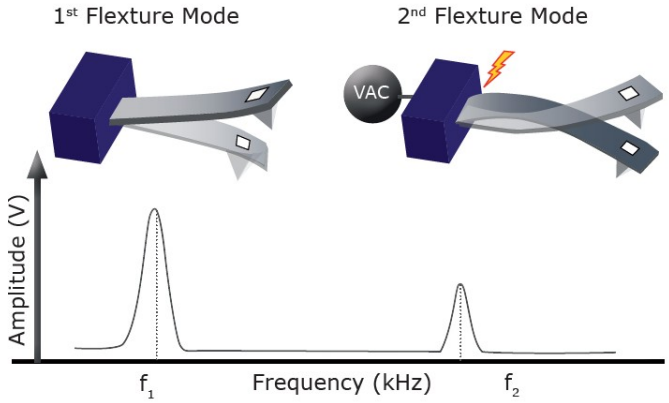

Figure 4: Concept of Bimodal HD-KFM: first flexural mode (or eigenmode) frequency is excited mechanically to measure to-pography, while the second flexural mode frequency is excited electrically to measure surface potential.

BIMODAL HD-KFM. HIGH SENSITIVITY AND ROBUSTNESS

Graphene has emerged as a nanomaterial for the future due to its bidimensional structure and electronic properties. However, synthesis and transfer processes are not easy to implement especially on large areas where a single layer of graphene may have impurities or flakes of multiple layers of graphene.

Although Raman spectroscopy is most commonly used to characterize monolayers of graphene, HD-KFM measurements have also proved to be useful to distinguish between single monolayer and multiple layers of graphene. Fig. 5 shows both topography (Fig. 5a) and HD-KFM surface potential images (Fig. 5b) of a graphene on Si sample. An ANSCM-PT probe (AppNano, USA) with an spring constant of 3 nN/nm was used. The imaging parameters were A_{01} = 18.5nm, A_{SP1} = 18nm, A_{02} = 1.9nm, A_{SP1} = 1.6nm. In the topographic image, it can be seen an aggregate of several flakes which form nearly a cont-inuous film. Some areas show higher height values due to multiple layer stack or self bending of the layers (white stripes in the image). Simultaneously, the surface potential image (Fig 5b.) provides information of the layers with higher contrast.

Silicon oxides areas are depicted as red areas (with the colored-scale choosen). The graphene monolayers correspond to the blue areas, double layer to green areas and triple layers of graphene appear as orange areas. In addition, it can also seen that some single monolayer areas in the bottom corner of the structure have slightly higher potential values (notice the dark blue color) which can also indicate some surface charging of the SiO_2 substrate below the graphene monolayer.

Another channel typically used in resonant mode is the phase signal, which is related to energy dissipation mechanisms between tip and sample. Image 5c shows the corresponding phase signal channel obtained simultaneously to the surface potential, where no contrast among different layers is shown, only between substrate and graphene aggregate.

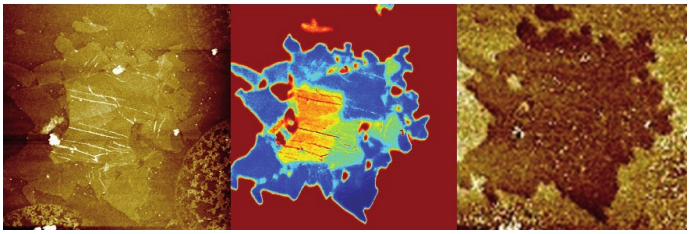

Figure 5: Topgography (a), surface potential (b) and phase (c) channels of a graphene aggregate on SiO2 substrate showing flakes of 1, 2 and 3 layers.

Another example of the high sensitivity and resolution is shown on Fig. 6 on a sample of graphene over silicon carbide (SiC). Fig. 6a shows the topography which shows the typical morphology of multiple atomic terraces of SiC.

Some of these terraces are covered with graphene layers but are not clearly distinguished in the topography image due to the height variations of the sample. However, the surface potential image (Fig. 6b) obtained with HD-KFM clearly separates both materials: grey depicted areas correspond with SiC areas while orange depicted areas correspond with surface covered with a monolayer (ML) of graphene. Moreover, there are small yellow regions which corresponds with areas covered by a double-layer of graphene or bi-layer (BL). As in the example shown in Fig. 5, surface potential of graphene increases with the number of layers.

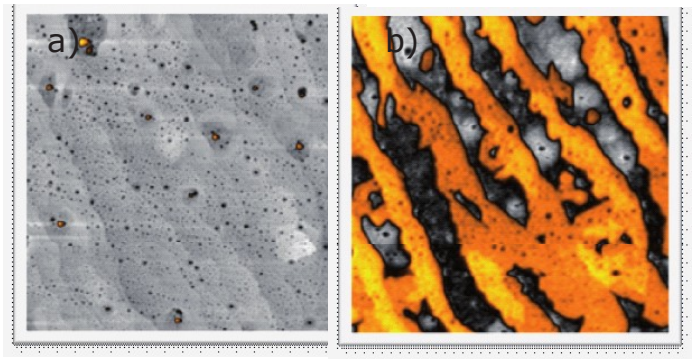

Figure 6 : Topography (left) and surface potential (right) of a graphene on silicon carbide substrate (SiC). Topography shows typical stepped-morphology of silicon carbide.
Presence of graphene layers is not well defined due to the high dynamic range of the scanned area. However, surface potential provides a way to distinguish between SiC (grey areas) and graphene layers (orange areas). Moreover, second layers can be found, the signal is still stable enough.

Another bidimensional material which has an increasing interest as an active electronic material is molybdenum disulphide (MoS_2). As compared to graphene, MoS_2 shows semiconductor properties which make it more interesting for devices like transistors or solar cells. In Fig. 7a and 7b, are shown both topography and surface potential (SP) images of a flake of MoS_2 transferred onto a gold sample.

Topography shows the presence of several terraces with different heights. This material shows, like in the case of graphene, a strong dependence of the SP with the number of layers as can be seen by comparing both images.

However, in the case of molybdenum disulphide, SP decreases with the number of layers. It is also interesting to notice that the gold substrate is covered by organic contaminants due to its high free surface energy, however they are not present on the surface of the MoS_2 flake.

Another bidimensional material which has an increasing.

interest as an active electronic material is molybdenum disulphide (MoS_2). As compared to graphene, MoS_2 shows semiconductor properties which make it more interesting for devices like transistors or solar cells. In Figures 7a and 7b, are shown both topography and surface potential (SP) images of a flake of MoS_2 transferred onto a gold sample.

Topography shows the presence of several terraces with different heights. This material shows, like in the case of graphene, a strong dependence of the SP with the number of layers as can be seen by comparing both images.

However, in the case of molybdenum disulphide, SP decreases with the number of layers. It is also interesting to notice that the gold substrate is covered by organic contaminants due to its high free surface energy, however they are not present on the surface of the MoS_2 flake.

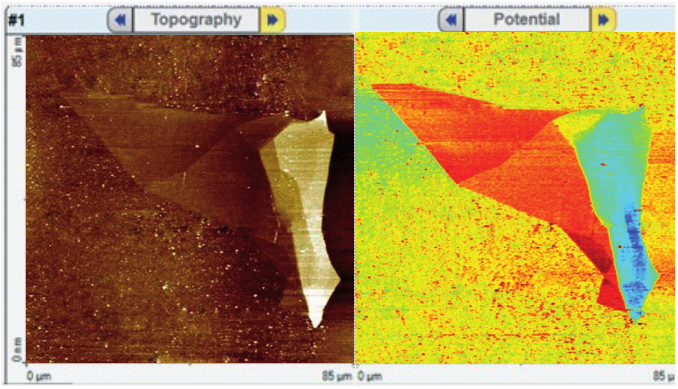

Figure 7: Topography (left) and surface potential (right) of a sample of molibdene disulfide on gold substrate. Topography shows layers of different height. Surface potential image (right) shows the corresponding SP value of each layer. On the contrary to the graphene case, SP decreases with the number of layers.

BIMODAL HD-KFM. HIGH ACCURACY AND SENSITIVITY TO DIFFERENT MATERIALS.

In order to test the accuracy of the surface potential values obtained with Bimodal HD-KFM, a standard sample test for KFM was imaged. This sample consists of a silicon substrate with two different metals (Gold and Aluminum) regions of 100 nm height defined by lithography. It is easy to find a region where three different materials are exposed (Gold-Silicon-Aluminum) thus, defining clear regions for the surface potential image. Fig 8. shows a 3D representation of this area with an overlapping of the of the corresponding surface potential image(different colors indicate different SP value). Every material can be clearly distinguished in the SP image with enough resolution as can be seen in the histogram of the colour-scale bar on the right side. Fig. 9 shows both topography and SP images and a cross-section. It is important to notice that the SP cross-section (white line) shows no bending due to capacitive influences of tip and cantilever or averaging with the surrounding areas (Au and Al regions are 100 nm high). Even more, HD-KFM shows its high sensitivity as an intermediate region between silicon and Aluminum can be resolved. This region might be an effect of the lithography process or the fabrication of the sample as the topography reveals that the Aluminum area is not as flat as the gold area. The differences in the SP values between the Au-Si-Al areas are consistent with standard values of the work function for each material.

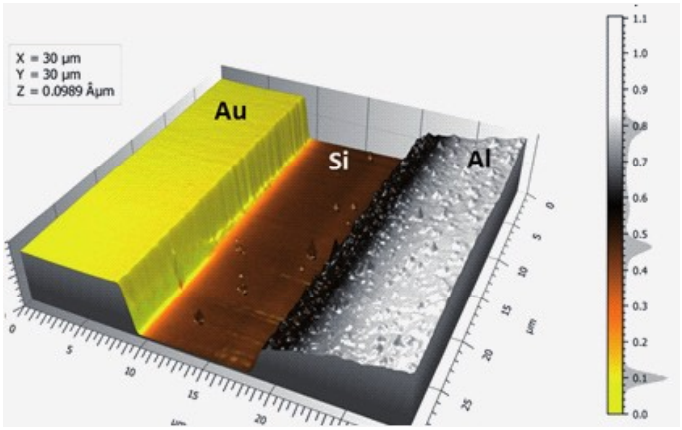

Figure 8: 3D view with colour overlay of surface potential values of a KFM test sample with well-defined Au-Si-Al regions measured in ambient conditions.

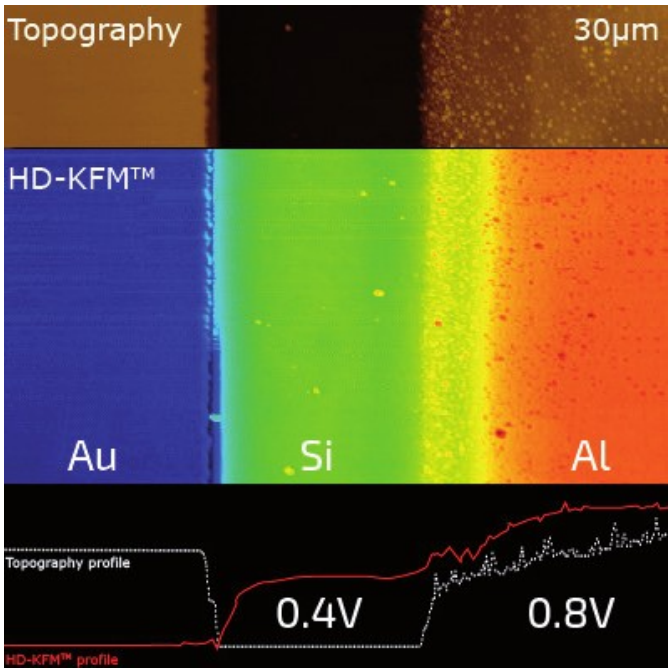

Figure 9: Topography (top), surface potential (middle) andcross-section (bottom) of the sample shown in Figure 7. High sensitivity of bimodal HD-KFM reveals a transition region between silicon and aluminum. Values are in good agreement with the bulk values of work functions.

In order to also test the accuracy and resolution of the HD-KFM on other materials, a sample of silver nanoparticles (courtesy of Prof. A. Colina, University of Burgos) was imaged with the HD-KFM mode. The NPs were electrochemically growth and then transferred to a silicon substrate. This sample has two well defined materials (Si and Ag): Si is the substrate reference while Ag NPs are easily recognized due to their triangular and hexagonal geometry. In addition, this sample is a good test for lateral resolution, as NPs of less than 200 nm can be found on the surface. An ANSCM-PT probe (AppNano, USA) with a spring constant of 3 nN/nm was used. The imaging parameters where A_{01} = 14.3 nm, A_{SP1} = 13.9nm, A_{02} = 1.2nm. Figure 10 (left and right) shows both topography and surface potential respectively. The smallest silver nano-triangles found in the image have a side length of 150 nm, which is about 5 times the nominal tip radius for this type of probes. Even so, some small domains of 50 nm-60 nm can be measured on the vertices of some nano-triangles. These spots, could correspond with a nucleation site of another nanoparticle.

The inset in the topography image corresponds to the histogram of surface potential image values and has a centred peak-to-peak difference of 430 mV higher in the silver NPs respect to the silicon substrate.
This value is consistent with a theoretical value calculated from standard values of the work function of both materials (Ø Si> Ø Ag). In HD-KFM, the bias is applied to the tip so that the surface potential difference between silver NPs and silicon would be:

$$V_{POT_{Ag-Si}} = \frac{\Delta\varphi Ag}{e} - \frac{\Delta\varphi Si}{e} = \frac{\varphi_{tip}\ \varphi_{Ag}}{e} - \frac{\varphi_{tip}\ \varphi_{Si}}{e} = \frac{\varphi_{Si}\ \varphi_{Ag}}{e} = \frac{4.85eV - 4.26eV}{e} = 590\ mV$$

This value has been calculated with the work function for poly-crystalline silver, however for crystalline silver oriented to 110 direction this value would be 330mV, thus indicating that the silver NPs might be mixture of polycrystalline and crystalline domains.

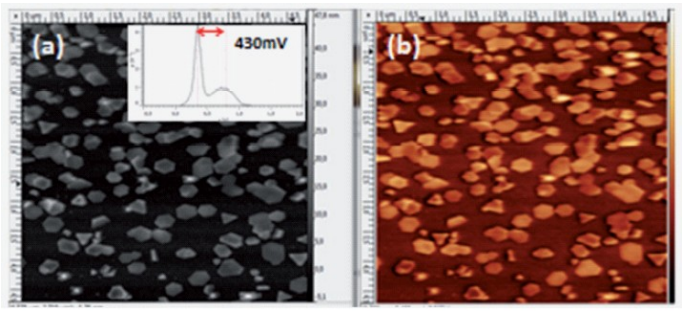

Figure 10: Topography (left) and surface potential (right) images of Au nanoparticles of 70-200nm on a silicon substrate. The inset on the topography image shows the histogram of SP values with an average difference between silicon and gAu of 430mV.

As mentioned above, Bimodal HD-KFM has a higher sensitivity due to the capability to probe the electric field very close to the surface. This is of vital importance when probing the SP of small objects like carbon nanotubes.
In the example shown in Fig. 11, a sample of carbon nanotubes was deposited on a silicon substrate by dropcasting from a di-luted solution. The length of the carbon nanotubes ranges from 1-10µm randomly oriented over the surface. The SP corres-ponding to the silicon surface is 295mV, while for the corres-ponding nanotubes it drops to 39mV as shown in Fig. 11(right). The apparent width of the carbon nanotubes in the SP image is 30nm, which is due to a convolution effect of the conductive tip. Additionally it can be seen the presence of small contami-nants on top of the carbon nanotubes as shown in Fig. 11(left). This can obscure the SP signal for high concentration (red arrows) but not for small concentrations (blue arrows). Even in the worst case, with Bimodal HD-KFM the signal is not comple-tely lost. This signal could not be probed by using a double-pass setup as the signal would be lost with the lift separation.

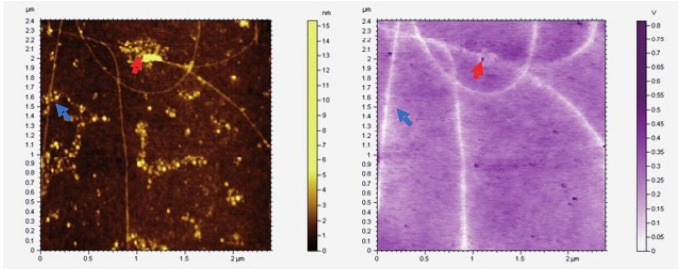

Figure 11: Topography (left) and surface potential (rigth) of a dropcasted sample of nanotubes. HD-KFM is sensitive enough to probe the surface potential signal of the nanotube even with the presence of contaminants covering it.

BIMODAL HD-KFM IN ORGANIC AND POLYMER SAMPLES

Surface potential can also be used to characterize organic and polymer materials.

Fig. 12 shows topography (left) and surface potential (right) of a film of polystyrene deposited on top of a silicon substrate by spin-coating. For small velocities and concentrations the film looks to be discontinuous, forming small aggregates and some regions with coalesced aggregates. However, there are also some regions with films of polystyrene that could be in a crystalline or semi-crystalline phase. In this state, they could accumulate charges that are measured on the surface potential image with higher values of the surface potential as compared to the more amorphous phase.

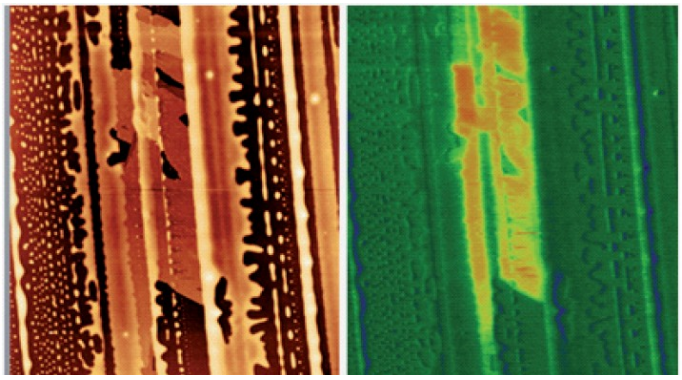

Figure 12: (Left) topography of spin-coated film of polystyrene (PS) over silicon. (Right) Surface potential image. There is no SP contrast between the aggregates of PS and the substrate, except for some small regions that could correspond to a more crystalline phase.

Another type of organic molecules, fluoroalkanes $F_{14}H_{20}$ were also characterized by HD-KFM. This sample was prepared by spin cast of a small droplet dissolved in perfluorodecalin on a Si substrate. By controlling the concentration, they are adsorbed onto the surface forming small toroids of few nanometers diameter. Fig. 13 shows both topography (left)and SP (right) images. HD-KFM show a difference in the surface potential of -0.2V in respect to the silicon substrate, which results from its well-defined dipole between the fluorinated parts with negative charge and carbon parts with positive charge. Although this value has been reported higher in the literature, it can be attributed to a deformation of the structure of the chain, so that the effective dipoles are tilted. A negative value indicates that the fluorinated parts are facing the tip. Also, the difference in lateral resolution of the individual molecules in both topography and SP images can be seen. The apparent size in topography is about 49.3nm average, while in the SP image it is 64.7nm. This can be attributed to the fact that the tip radius of the cantilever used in the experiments (ANSCM-Pt, AppNano) is about 20-30 nm. However, the topography image is based on the surface interaction which is more localized than the electric interaction. That is why the inner part of the donut-shaped molecules is resolved in topography, while in the SP image it is not resolved. Also in the molecules that are closer, there is a small increase of the signal in the borders (tiny white lines along the contour). This is due to the addition of the electric signal of dipoles of two adjacent molecules (see the screen in the inset of Fig. 13b). Using a conductive tip with higher aspect ratio, it would increase the lateral resolution also in the SP image.

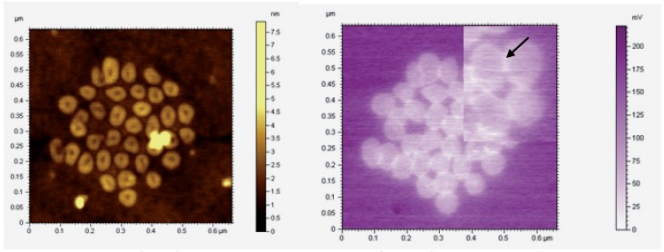

Figure 13: (left) topography and (right) surface potential of fluoroalkenes molecules. Topography shows higher lateral resolution due to capactive effects of the tip which enlarge the effective interaction area. Also, a white contrast is observerd in the borders of adyacent molecules which could be due to the overlap of the dipoles field of the surrounding molecule.

Another example of the high lateral resolution that can be achieved with Bimodal HD-KFM is shown in Fig. 14. A sample of highly oriented pyrolytic graphite (HOPG) was used to deposit biomolecules on the surface. This molecules form a self assembled monolayer (SAM) with a pitch of 10nm between lines of parallel-arranged molecules.

Fig. 14 (left) shows topography and Fig. 14 (right) shows the surface potential. The presence of a SAM of biomolecules is clearly appreciated in the topography image on the terrace situated on the right side. Bimodal HD-KFM shows an SP average value of 208mV for HOPG terraces not covered by biomolecules. On the SAM, the SP value drops to 126 mV.

It is important to notice that SP image also resolves the pitch between molecules as shown in topography, thus indicating the high lateral resolution that can be achieved with bimodal HD-KFM.It is also interesting to point out that the presence of biomolecules is also sensed by the SP image in the bottom terrace next to the SAM as the SP values are similar; however, it is not noticeable in the same area in the topographic image (indicated by blue arrows)

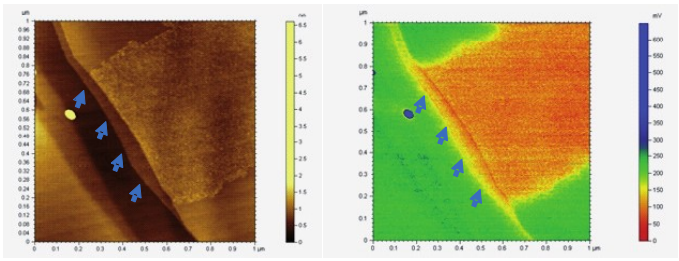

Figure 14 : Topography (left) and SP (right) of a sample of HOPG with a SAM of biomolecules on it. High resolution SP image shows the 10 nm pitch between arranged molecules and also the presence of a second SAM on a lower HOPG terrace that is not resolved in the topographic image.

BIMODAL HD-KFM ON ELECTRONIC DEVICES AND SOLAR CELLS

Fig. 15 shows an electric characterization of a perovskite solar cell made with HD-KFM mode with a Nano-Observer AFM. In Fig. 15 (left) there is a picture of the positioning of the tip in the edge of a cleaved solar cell growth on a glass substrate. Due to the difficulty in making a good cleavage of the glass, high resolution side view is crucial to place the tip in a good region for AFM measurements and close to the edge, where the active layers of the solar cell are located. Fig. 15 (middle and right) shows the corresponding surface potential images and cross-section as described in Castillejo et al. APL 2014.

To our knowledge no other publication has shown a surface potential profile of the active layer of a solar cell without polishing the solar cell after cleaving it, so that the active layers are not further modified. Bimodal HD-KFM is the only commercially available mode robust and sensitive enough to provide reliable surface potential measurements even on a sample with high topographic variations.

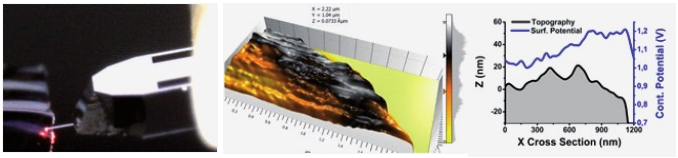

Figure 15: (left) lateral view of the positioning of the cantilever on the edge of the solar cell. (middle) 3D reconstruction of the edge of the solar cell with coloured overlay of the surface potential. (right) cross-section of the edge of the solar cell.

It is also interesting to measure a solar cell that has been polished as shown in Figure 17 where both topography (Fig.16-top) and surface potential (Fig. 16-bottom) are shown. Some different layers can be seen on topography despite the polishing process, however, surface potential shows the actual position of the active layers. Moreover, on the right side of the surface potential image it can be seen some defects in the active layers that could be due to the polishing process (red arrows in the surface potential image). This small defects are about 50-70nm size, showing the high resolution provided by the bimodal HD-KFM.

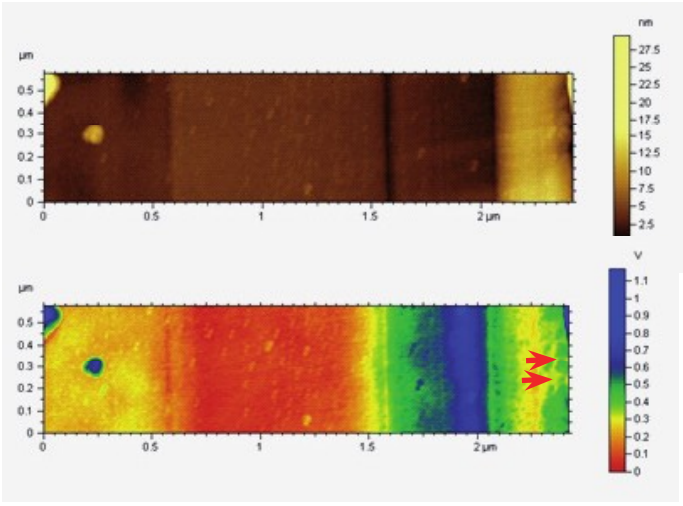

Figure 16: Topography (top) and surface potential (bottom) of a polished solar cell.

As mentioned above, there is a growing interest on using 2-D materials for substituting standard materials on electric devices. Fig. 17 shows several devices consisting of gold pads connected by a graphene membrane with different separation lengths between the pads. Graphene membranes are transferred by using a PDMS stamp and after that, gold pads are grown by lithography. After electrical characterization by current measurement flow between the pads, some devices are found to be defective. A surface potential map obtained with HD-KFM reveals that this is due to the presence of oxidation on the surface (blue areas on the SP image). This oxidation was found to occur because of the transferring process with PDMS stamp which may release some solvents onto the surface. As the current is made to flow to test the device, this areas become oxidized. In this case, topography is not sensitive enough to detect the presence of oxide areas on the substrate, however, HD-KFM is highly sensitive to it.

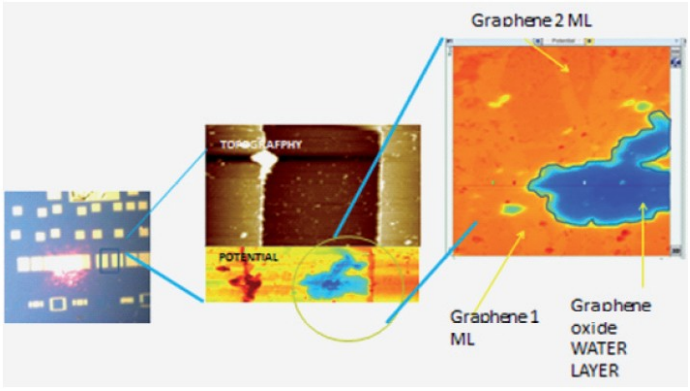

Figure 17: (left) Optical micrograph of electronic devices based on graphene. (middle) topography and surface potential of one of the devices. (right) zoom of the SP image of an area where a large oxide region is seen. This oxide can be originated by rests of solvent of the PDMS stamp used to transfer graphene membranes.

CONCLUSIONS

Electric characterization with the atomic force microscope has an increasing demand among the AFM community to solve new research topics in nanotechnology like energy harvesting, polymer or organic based electronics, or new advances in the semiconductor industry. This article described several applications of surface potential characterization with bimodal HD-KFM. This technique developed by CSI for the Nano-Observer AFM has the advantage of amplifying the feedback signal through the second eigenmode of the cantilever. Also it allows a much closer probe of the electric field created by the surface potential compared to other approaches. This is of extreme relevance when imaging small molecules or bidimensional materials.

BIBLIOGRAPHY

1. D.W. Abraham, C. Williams, J. Slinkman, H.K. Wickramasinghe, J. Vac. Sci. Technol. B 9,703 (1991)

2. T.R. Albrecht, P. Gr¨utter, D. Horne, D. Rugar, J. Appl. Phys. 69, 668 (1991)

3. T. Glatzel, S. Sadewasser, R. Shikler, Y. Rosenwaks, and M. C. Lux-Steiner, Mater. Sci. Eng. B 102(1–3), 138–142 (2003).

4. J. Colchero, A. Gil, A.M. Bar´o, Phys. Rev. B 64, 245403 (2001).

5. A. Liscio, V. Palermo, and P. Samorı, Adv. Funct. Mater. 18(6), 907–914 (2008).